

# Status of polarized structure functions

*Claude Marchand*

CEA, Centre de Saclay, IRFU/SPhN, 91191 Gif-sur-Yvette, France

DOI: <http://dx.doi.org/10.3204/DESY-PROC-2012-02/20>

An experimental overview on polarized structure functions of the nucleon is given. It covers results from experiments performed at CERN, HERA, JLAB and RHIC. Latest results on quark and gluon helicities are discussed, as well as results on Transverse Momentum Dependent distribution functions (TMD).

## 1 Introduction

At leading order in pQCD, lepton-nucleon or proton-proton scattering at high energies can be interpreted as photon-quark (gluon) or quark-quark (gluon) scattering during a fragmentation phase, followed by the dress up of the quark to form a meson or a hadron in the final state. It allows thus to study quark (gluon) distribution functions (DF), given the quark fragmentation function (FF) is known. In collinear approximation (i.e. integrating over intrinsic transverse quark momentum  $k_T$ ), the leading twist contribution to the quark distribution (density) function can be written as ([1]):

$$\Phi(x) = \frac{1}{2} \{q(x) + \gamma_5 \Delta q(x) S_L + \gamma_5 \Delta_T q(x) S_T \gamma_1\} n^+$$

Here, in conventional notations,  $q(x)$  represent the unpolarized quark distribution function,  $\Delta q(x)$  the longitudinal polarized quark distribution function (also called helicity), and  $\Delta_T q(x)$  the transversely polarized quark distribution function. In the non relativistic limit,  $\Delta_T q(x) = \Delta q(x)$ .

One of the main goals of the current experiments studying nucleon spin structure is to determine how the total longitudinal spin projection of the nucleon,  $1/2$ , is distributed among its constituents, quarks, gluons and orbital angular momentum:

$$\frac{S_z^N}{\hbar} = \frac{1}{2} = \frac{1}{2} \{ \Delta \Sigma (= \sum_q \Delta q) + \Delta G + L_z^q + L_z^g \}$$

We review here the recent results on the gluon and quark helicities obtained by HERMES, COMPASS, PHENIX and STAR experiments. Measurements of transverse spin asymmetries, leading to the determination of the transverse spin quark distributions and to the Sivers functions obtained by HERMES and COMPASS are also discussed, as well as their possible relation to Orbital Angular Momentum (OAM).

## 2 Longitudinal spin structure of the nucleon

Based on all the world data ([2, 3] and references therein) were the structure functions  $g_1^p(x, Q^2)$  and  $g_1^d(x, Q^2)$  have been obtained in inclusive Deep Inelastic Scattering (DIS) (Fig. 1), and

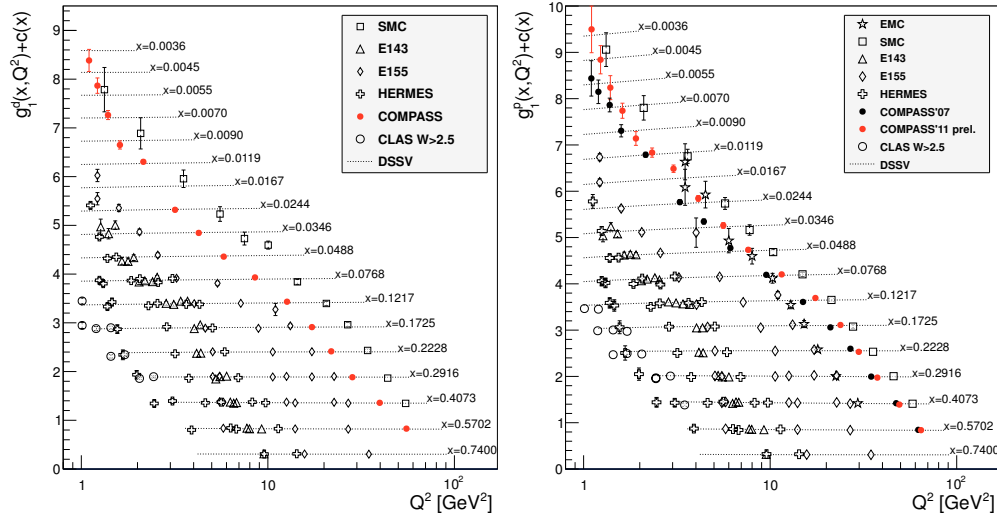


Figure 1: World data on  $g_1^d$  (left) and  $g_1^p$  (right), compared to global fit of DSSV [4]. Also shown for  $g_1^p$  are preliminary data obtained in 2011 at COMPASS with 200 GeV muon beam.

using additional information from neutron and hyperon decays ( $a_3$ ,  $a_8$ ), the sum of the quark contribution to the nucleon spin (in  $\overline{MS}$ ,  $\Delta\Sigma = a_0$ ) turns out to be about 33% [4]. In addition to the quark helicities, it is thus important to study also the gluon helicities, as well as the Orbital Angular Momentum (OAM), in order to hope solving this so called spin crisis.

## 2.1 Quark helicities

As seen above, inclusive DIS gives already a lot of information on the quark helicities, allowing to measure the sum of their contribution to the nucleon spin via  $\Delta\Sigma = \sum_{u, \bar{u}, d, \bar{d}, s, \bar{s}} \Delta q$ . Using in addition SU3 flavor symmetry, were one assumes  $\Delta\bar{u} = \Delta\bar{d} = \Delta\bar{s} = \Delta s$ , and the DGLAP evolution equations, one can obtain separate information on the valence quark ( $\Delta u_v(x)$ ,  $\Delta d_v(x)$ ) and sea quark ( $\Delta\bar{q}(x)$ ) helicities, as well as the gluon helicity  $\Delta G(x)$  [5]. However, as the world coverage in  $Q^2$  range is small, specially at low  $x$ , the accuracy on  $\Delta G$  is bad. So more direct measurements of  $\Delta G$  are needed. Also, from  $g_1^p$  and  $g_1^d$  alone, with the knowledge of  $a_3$  and  $a_8$ , one can obtain with simple algebra, the contribution of the strange quarks to the nucleon:  $(\Delta s + \Delta\bar{s}) = \frac{1}{3}(a_0 - a_8) = -0.08$  [6].

Nevertheless, in order to be able to access to the quark distributions separately for  $u, d, s, \bar{u}, \bar{d}$  and  $\bar{s}$ , it is necessary to study semi-inclusive DIS (SIDIS) channels, where in addition to the scattered probe, also a hadron is detected in the final state. In this case, in LO in pQCD, the measured asymmetries can be written as a sum of products of quark distribution functions  $\Delta q(x, Q^2)$  and fragmentation functions  $D_q^h(z, Q^2)$ ,  $z$  being the fraction of the probe momentum carried by the emitted hadron  $h$ .

In parallel to the polarized inclusive DIS measurements, such semi inclusive (SIDIS) events where an additional hadron tags the flavor of the struck quark, were recorded both at HERMES and COMPASS [6, 7]. These data are used to extract at LO the helicity quark distributions for

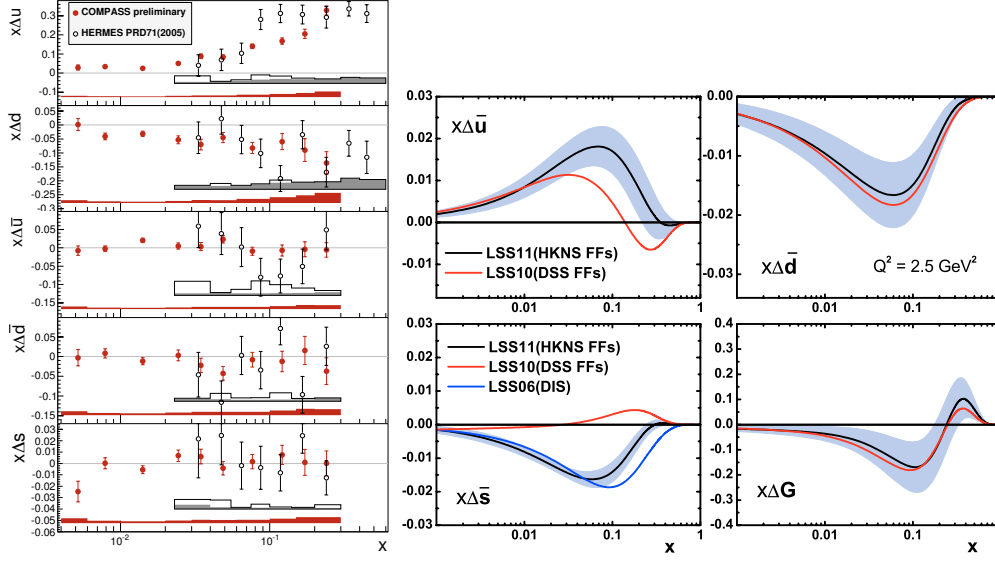


Figure 2: Left:  $\Delta q(x)$  measured from SIDIS data at COMPASS [6] and HERMES [7]; Right: Results from global fit [9] using different FF's.

each quark flavor separately down to  $x = 0.004$ . This provides a wider picture of the nucleon spin, however requiring as an additional input the quark fragmentation functions. COMPASS results [6] obtained using FF's from DSS [8] are shown in Fig. 2 together with HERMES results [7] where FF's are extracted from the same HERMES data. The curve shows the global QCD fit of DSSV [4] at LO. Sea quark polarized distributions are found to be compatible with zero within the statistical errors. Concerning the strange quarks, note that the DSSV fit accommodates both the SIDIS data (COMPASS and HERMES data, shown here and compatible with zero), and the results from analyses of inclusive DIS data, which lead to a negative first moment for  $\Delta s$  (suggesting a negative contribution at low  $x$ ). In the future, the SIDIS sector will benefit from more precise determination of quark FF's.

At RHIC, in a short exploratory run, first p-p collisions at 500 GeV were performed. By studying the parity violating reaction  $u + \bar{d} \rightarrow W^+ \rightarrow e^+ + \nu$ , the quantity  $\Delta \bar{d}/\bar{d} - \Delta u/u$  is probed. First results from PHENIX and STAR reporting asymmetries with signs as expected from SIDIS results, are very encouraging [10, 11]. The advantage of this channel is that no FF are needed for the extraction of quark helicities.

## 2.2 Gluon polarization

In addition to the method of global fits on DIS data using DGLAP evolution, described in section 2.1, there are two more direct ways to experimentally determine the gluon polarization.

The first method is via polarized lepton nucleon SIDIS reactions, where the double spin asymmetry of cross sections for the photon gluon fusion (PGF) process  $\gamma g \rightarrow q\bar{q}$  are measured. PGF events can be searched for in two channels: the “open charm channel” where a  $c\bar{c}$  pair is produced and a charm quark is identified via the production of a  $D^0$  meson, and the “high  $p_T$  hadron” channel, where outgoing quarks (likely light quarks) hadronize into hadrons, mainly

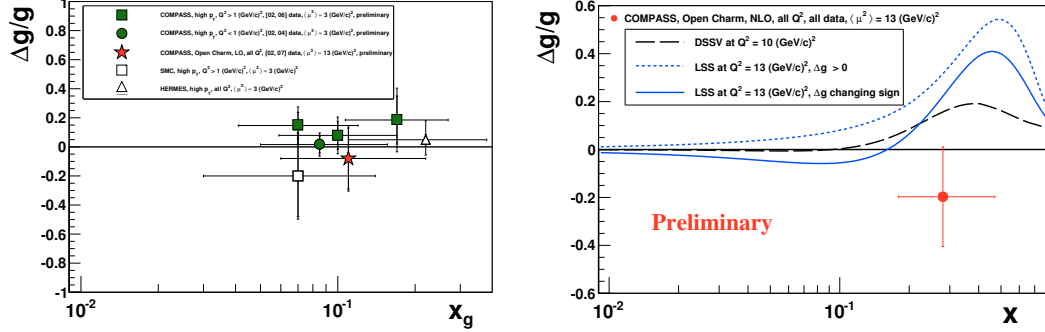


Figure 3: Direct measurements of  $\Delta G/G$  via Photon Gluon Fusion. Left: LO extraction from open charm [12] and high  $p_T$  [13, 14, 15] PGF; Right: first NLO extraction from open charm at COMPASS [14], compared to DSSV [8] and LSS [9] global fits

pions, with high transverse momentum  $p_T$ . The open charm channel is only accessible at COMPASS [12] thanks to the high energy of the CERN polarized muon beam. It provides a clean signature of the PGF, but is a difficult channel requiring to count events with  $D^0$  production over a large combinatorial background of  $\pi K$  pairs, leading to limited statistics. On the contrary, the high  $p_T$  channel, used at both COMPASS [13, 14] and HERMES [15], benefits from high statistics but suffers from competing background processes (leading order, QCD Compton, resolved photon) which have to be simulated and accounted for.

Figure 3 left shows all existing direct measurements of the gluon polarization  $\Delta G/G(x)$  extracted at leading order in QCD from the measured spin asymmetries in the high  $p_T$  and charm channels. COMPASS results from the open charm [12] (star) and high  $p_T$  [13, 14] (circle and closed square) channels are shown together with HERMES [15] (open triangle) and SMC (open square) results. Figure 3 right shows  $\Delta G/G(x)$  extracted at NLO from the COMPASS charm channels [14], compared to global QCD fits from DSSV [4] and LSS [9], which do not include these data. The measurements probe  $x_g$  values of the gluon momentum fraction around 0.1-0.2 and give results compatible with zero in this kinematic range. The accuracy of these data, as well as the limited  $x_g$  range covered, do unfortunately not allow to constrain with high enough accuracy the first moment of  $\Delta G$ , which enters in the nucleon spin decomposition.

The second method is via polarized hard  $\vec{p}\vec{p}$  collisions, by choosing channels sensitive to  $\Delta G$  and measuring double spin asymmetry of cross-sections. Such experimental studies of the gluon polarization have been performed at the RHIC collider. Collisions of protons polarized longitudinally in opposite directions have been realized mainly at  $\sqrt{s} = 200$  GeV, but also at 62 GeV and more recently 500 GeV, covering various kinematics ranges. Several channels are used to pin down the gluon polarization. The most abundant channels in term of statistics are the production of  $\pi^0$  at PHENIX [16] and the production of jets at STAR [17]. In both cases, three different elementary processes ( $gg$ ,  $gq$  and  $qq$ ) contribute to the cross-section, so that the measured double spin asymmetries  $A_{LL}$  are sensitive to a combination of three quantities:  $\Delta G(x_1)\Delta G(x_2)$ ,  $\Delta G(x_1)\Delta q(x_2)$ , and  $\Delta q(x_1)\Delta q(x_2)$ , where  $x_1$  and  $x_2$  are the fractions of momentum carried by the two colliding partons. For each physical channel ( $\pi^0$ ,

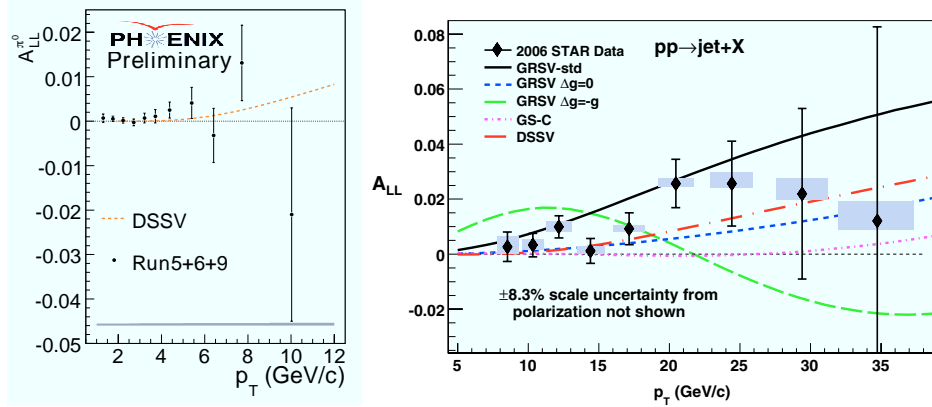


Figure 4: Double spin asymmetries measured at RHIC with  $\bar{p}p$  collisions at  $\sqrt{s}=200$  GeV compared to DSSV [4]. Left: for  $\pi^0$  production at Phenix [16]; Right: for single jet production at STAR [17].

jets, etc.) the measured double spin asymmetry  $A_{LL}(p_T)$  is compared to calculations where a given parametrization of  $\Delta G(x)$  is assumed. The results are presented in Fig. 4 left for the  $\pi^0$  channel measured at PHENIX [16] and right for the single jet channel measured at STAR [17]. Both data sets favor a parametrization with a gluon polarization close to zero. When re-injected in global QCD fits including in addition world DIS and SIDIS data [4], these data provide a strong constrain on the first moment of  $\Delta G$  truncated to the measured range  $0.05 < x_g < 0.2$ :  $\Delta G^{RHIC} = 0.005^{+0.129}_{-0.164} (\Delta\chi^2/\chi^2 = 2\%)$ . Without the constraint on the  $x_g$  range,  $\Delta G$  obtained by these fits turns out to be  $0.013^{+0.702}_{-0.314}$ , what can not fully rule out a sizeable contribution of  $\Delta G$  to the nucleon spin. Data taken at higher energy (500 GeV) will be helpful to constrain the lower  $x_g$  region.

### 3 Transversity and TMD

The understanding of the nucleon (spin) structure obtained by studying the quark helicities  $\Delta q$  is basically a one-dimensional one in longitudinal momentum space. Two complementary descriptions can provide tomographic images of the structure of the nucleon in terms of partons: one in the transverse plane in momentum space, through Transverse Momentum Dependent parton distributions (TMD) [18, 19]; one in the transverse plane in coordinate space, through the generalized parton distributions (GPD) [20, 21]. We will only focus here on TMD's.

In the non collinear case, that is not integrating over the quark transverse momentum  $k_T$ , there are eight leading twist TMD's for the nucleon [1], listed in Table 1 (we stick from now on to the notations of [1], notations adopted in section 2 are in parenthesis).

The unpolarized parton DF  $f_1(q)$  and the polarized parton DF  $g_1(\Delta q)$  have been discussed in section 2, and can be obtained in DIS. All other TMD's, including transversity TMD  $h_1(\Delta_T q)$  which is chiral odd, can only be accessed in SIDIS, or polarized DY and polarized p-p collisions. Except  $h_1$ , all other TMD would vanish in absence of parton OAM and are due to the coupling of parton transverse momentum to nucleon/quark spin. In (un)polarized SIDIS, where a spinless pion or kaon is produced in the final state, they can be obtained by the study of the following

$q_{pol.} \setminus N_{pol.}$	U	L	T
U	$f_1(q)$		$f_{1T}^\perp$
L		$g_1(\Delta q)$	$g_{1T}$
T	$h_1^\perp$	$h_{1L}^\perp$	$h_1(\Delta_T q)$
T			$h_{1T}^\perp$

Table 1: Eight leading twist TMD's classified as a function of quark and Nucleon polarizations

azimuthal modulations of single (SSA) or double (DSA) spin asymmetries [22], which are each sensitive to the convolution of a TMD with the corresponding fragmentation function (FF):

- Transversity:  $A_{UT}^{sin(\phi_h+\phi_S)} \propto h_1 \otimes H_1^\perp$
- Sivers:  $A_{UT}^{sin(\phi_h-\phi_S)} \propto f_{1T}^\perp \otimes D_1$
- Pretzelosity:  $A_{UT}^{sin(3\phi_h-\phi_S)} \propto h_{1T}^\perp \otimes H_1^\perp$
- Boer-Mulders:  $A_{UU}^{cos(2\phi_h)} \propto h_1^\perp \otimes H_1^\perp$
- Worm-Gears:  $A_{UL}^{sin(2\phi_h)} \propto h_{1L}^\perp \otimes H_1^\perp$ ;  $A_{LT}^{cos(\phi_h-\phi_S)} \propto g_{1T}^\perp \otimes D_1$

Here, first and second subscripts in the labeling of the SSA or DSA indicate the beam and target polarization (U: unpolarized, L: longitudinal and T: transverse).  $\phi_S$  and  $\phi_h$  represent the azimuthal angles of the initial nucleon spin and the produced hadron momentum; they are defined w.r.t the direction of the virtual photon in the lepton scattering plane.  $D_1$  represents the unpolarized  $k_T$  dependent FF, and  $H_1^\perp$  the Collins FF, which describes the distribution of unpolarized hadrons in the fragmentation of a transversely polarized quark.  $H_1^\perp$  is chiral odd, and represents the ideal partner of transversity.

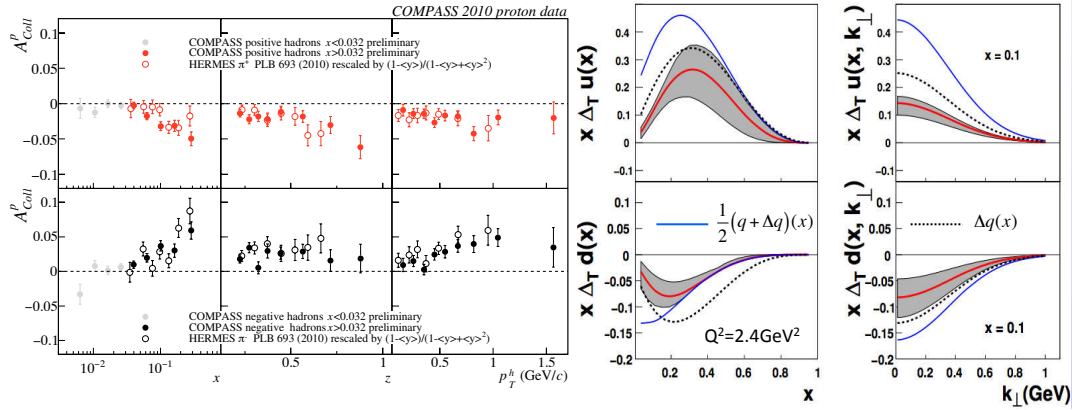


Figure 5: Left: Collins asymmetry  $A_{UT}^{sin(\phi_h+\phi_S)}$  measured on the proton in 2010 at COMPASS [25] compared to the ones obtained at HERMES [23]; Right: Transversity DF obtained by global analysis [30] of Collins asymmetries [23, 26] and FF [28].

### 3.1 Transversity and Collins asymmetry

The only way to access the transversity distribution  $h_1$  is by coupling it to another chiral-odd quantity. To such a purpose one can look for a chiral-odd partner either in the initial or the final state. In the first case the most promising approach, and the cleanest one from the theoretical point of view, is the study of the double transverse spin asymmetry,  $A_{TT}$ , in polarized Drell-Yan processes. Meanwhile, the most accessible and fruitful channel is the azimuthal asymmetry  $A_{UT}^{sin(\phi_h+\phi_S)}$  in SIDIS processes, namely  $lp^\dagger \rightarrow lhX$ , involving the convolution of the transversity distribution with the Collins fragmentation function. The Collins asymmetry is sensitive to the correlation between the outgoing hadron direction and the initial quark transverse spin, and can thus provide a determination of the quark transverse spin distributions  $\Delta_T u$  and  $\Delta_T d$ .

Collins asymmetries were measured both at HERMES [23] and COMPASS [24, 25] using a transversely polarized proton target, and in addition at COMPASS [26] using a deuteron target. Mainly because of cancelations between u and d quark contributions, the data on deuteron give asymmetries compatible with zero for Collins. This is also the case for data obtained at JLAB on a transversely polarized  $^3\text{He}$  target (neutron) [27]. On the contrary, signals are observed with the proton target for the Collins asymmetry for all charged hadrons, increasing as a function of  $x$ . New 2010 COMPASS data on the proton [25] are in excellent agreement with HERMES data, as can be seen in Fig. 5 (left), what implies a negligible  $Q^2$  dependence of the Collins effect. A crucial breakthrough has been achieved thanks to the independent measurement of the Collins function (or rather, of the convolution of two Collins functions), in  $e^+e^- \rightarrow h_1 h_2 X$  unpolarized processes by the BELLE Collaboration at KEK [28] (confirmed since by BABAR [29]). A combined fit [30] of the SIDIS data from HERMES on the proton [23] and COMPASS on the deuteron [26], together with the  $e^+e^-$  BELLE data [28], allowed the simultaneous extraction of  $\Delta_T u$  and  $\Delta_T d$ , with the interesting byproduct that the Collins unfavored fragmentation function is opposite to and as large as the favored one. As seen in Fig. 5 (right), they are opposite to each other in sign, and smaller in size than the helicity distributions. Including new 2010 COMPASS data on the proton [25] will help to improve this global fit.

An alternative method to probe quark transverse spin distributions  $\Delta_T u$  and  $\Delta_T d$  is to study azimuthal asymmetries from hadron pairs. Data from HERMES [31] and COMPASS [32] confirm the signal of transversity at high  $x$  observed in single hadron SIDIS. Combining these data with the Interference FF  $H_1^\perp$  measured at BELLE [33], a first direct extraction of  $(\Delta_T u - 1/4\Delta_T d)$  at LO has been performed [34], which is fully compatible with the results of the global fit on single hadron SIDIS [30]. A similar approach with hadron pair production is followed at PHENIX [35] by studying di-hadron correlations in p-p scattering at RHIC.

### 3.2 Sivers TMD and connection to OAM

The Sivers TMD, which correlates the nucleon spin and the transverse momentum of the parton  $k_T$ , was originally proposed to explain the large single-spin asymmetries observed in hadron-hadron scattering. The Sivers function is T-odd, namely it changes sign under naive time reversal. For a long time the Sivers function and the corresponding asymmetry were believed to vanish due to T-invariance arguments. One of the main theoretical achievements of the recent years was the discovery that the Wilson-line structure of parton distributions, which is necessary to enforce gauge invariance of QCD, provides the possibility for non-zero T-odd transverse momentum dependent (TMD) PDFs. FSI (or ISI for DY) allow for non zero Sivers functions, but they must have opposite signs in SIDIS and DY.

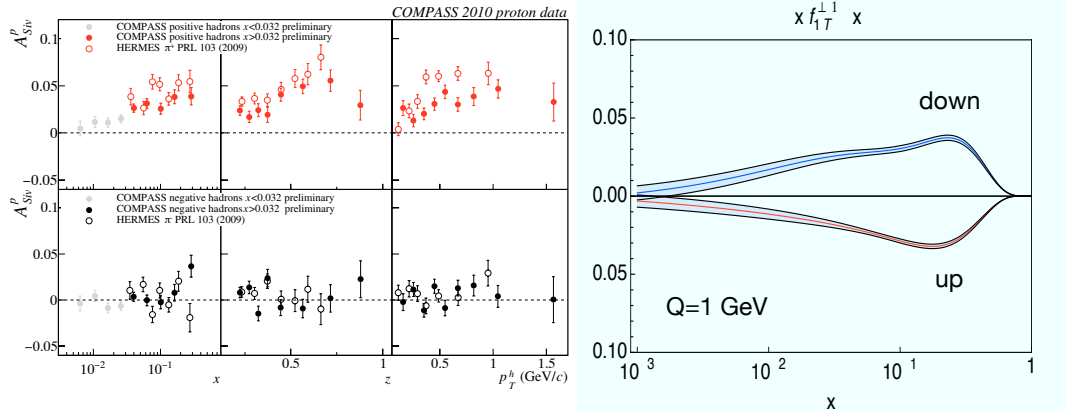


Figure 6: Left: Sivers asymmetry  $A_{UT}^{sin(\phi_h - \phi_S)}$  measured on the proton at COMPASS [25] compared to the ones obtained at HERMES [36]; Right: Extracted  $x.f_{1T}^\perp$  for u and d quarks [39].

Sivers asymmetries were measured in SIDIS at HERMES [36] and COMPASS [24] using a transversely polarized proton target, at COMPASS [26] using a deuteron target, and at JLAB on a  $^3\text{He}$  target (neutron) [27]. Mainly because of cancelations between u and d quark contributions to the isoscalar target, the data on deuteron give Sivers asymmetries compatible with zero. On the contrary, clear signals are observed on the proton target for the Sivers asymmetry for positive hadrons, while they are compatible with zero for negative hadrons. COMPASS data on the proton [25] give smaller signal than HERMES [36] (Fig. 6), which indicates a  $Q^2$  dependence of the Sivers TMD well accounted for by recent calculation of [37].

Global analysis [38, 39] using the HERMES proton data combined with the COMPASS deuteron data led to the extraction of Sivers TMD  $f_{1T}^\perp$  for u and d quarks, which turn out to be non zero, and of opposite sign (Fig. 6 right). Based on results of spectator models, a relation between Sivers TMD and the GPD E in the forward limit allows to constrain quark OAM using Ji's relation. Strikingly, the results are in agreement with other totally independent estimates [39].

### 3.3 Boer-Mulders and Worm-Gear TMD's

The Boer-Mulders TMD  $h_1^\perp$ , like the Sivers one, is naive T-odd and obeys thus the same rule that it has to change sign between SIDIS and DY. It originates from the coupling of the quark intrinsic transverse momentum and intrinsic transverse spin, a kind of spin-orbit effect, and can be accessed in conjunction with Collins FF via the  $\cos(2\phi)$  modulation of the unpolarized SIDIS reactions. This azimuthal asymmetry  $A_{UU}^{cos(2\phi_h)}$  has been measured for positive and negative hadrons produced in SIDIS on a unpolarized proton target at HERMES [40] and on a deuteron target at COMPASS [41]. HERMES data show large non zero signals for kaons, zero for  $\pi^+$  and positive for  $\pi^-$ . COMPASS show positive signal for both  $h^+$  and  $h^-$ . However, it could well be that twist-4 Cahn effect has a non negligible contribution to the measured  $\cos(2\phi)$  asymmetry.

The Worm-Gear TMD's  $g_{1T}^\perp$  ( $h_{1L}^\perp$ ) describe the probability of finding a longitudinally (transversely) polarized quark inside a transversely (longitudinally) polarized nucleon. Interestingly,

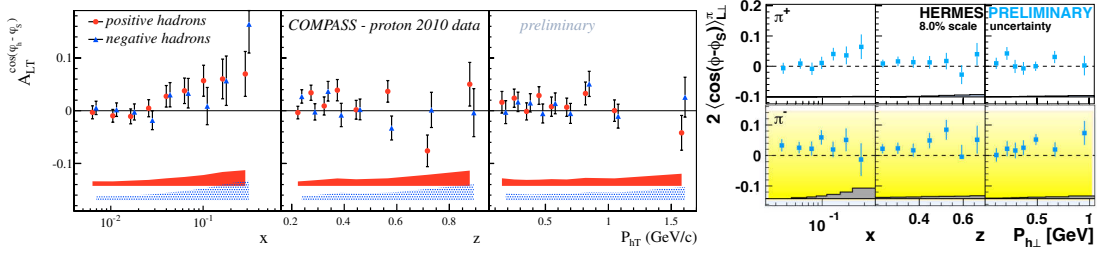


Figure 7: Preliminary  $A_{LT}^{cos(\phi_h - \phi_S)}$  measured on the proton at COMPASS in 2010 (left) and at HERMES [43] (right).

they are the only two leading-twist TMD's whose corresponding GPD vanish in light-cone quark models, and are found to be one the opposite of the other in these models. These two TMD's have however a different behavior under chiral transformations:  $h_{1L}^\perp$  is chiral-odd and can be probed in SIDIS in combination with the Collins FF, while  $g_{1T}^\perp$  is chiral-even and can thus be accessed in SIDIS combined with the unpolarized FF. In SIDIS experiments,  $g_{1T}^\perp$  can be accessed at leading-twist through the measurement of the DSA  $A_{LT}^{cos(\phi_h - \phi_S)}$ . Preliminary results exist using longitudinally polarized lepton beams on a transversely polarized proton target from COMPASS [42] and HERMES [43], and from JLAB on a  $^3\text{He}$  target [44]. A clear hint of a positive signal is found for the negative pions (hadrons) in all data sets, and even for positive hadrons with the new data taken in 2010 at COMPASS.

## References

- [1] P. J. Mulders, Progress in Particle and Nuclear Physics **55** (2005) 243.
- [2] COMPASS Collab., M. Alekseev *et al.*, Phys. Lett. **B680** (2009) 217.
- [3] COMPASS Collab., M.G. Alekseev *et al.*, Phys. Lett. **B690** (2010) 466.
- [4] D. de Florian, R. Sassot, M. Stratman and W. Vogelsang, Phys. Rev. **D80** (2009) 034030.
- [5] J. Blümlein and H. Böttcher, arxiv:1101.0052 [hep-ph].
- [6] COMPASS Collab., M.G. Alekseev *et al.*, Phys. Lett. **B693** (2010) 227.
- [7] HERMES Collab., A. Airapetian *et al.*, Phys. Rev. **D71** (2005) 012003.
- [8] D. de Florian, R. Sassot, and M. Stratman, Phys. Rev. **D75** (2007) 114010.
- [9] E. Leader, A. V. Sidorov and D. B. Stamenov, Phys. Rev. **D84** (2011) 014002.
- [10] PHENIX Collab., A. Adare *et al.*, Phys. Rev. Lett. **106** (2011) 062001.
- [11] STAR Collab., M. Aggarwal *et al.*, Phys. Rev. Lett. **106** (2011) 062002.
- [12] COMPASS Collab., M.G. Alekseev *et al.*, Phys. Lett. **B676** (2009) 31.
- [13] COMPASS Collab., E. S. Ageev *et al.*, Phys. Lett. **B633** (2006) 25.
- [14] COMPASS Collab., M. Stolarski, AIP Conf.Proc. **1441** (2012) 244.
- [15] HERMES Collab., A. Airapetian *et al.*, J. High Energy Phys. **1008** (2010) 130.
- [16] PHENIX Collab., A. Manion, J. Phys. Conf. Ser. **295** (2011) 012070.
- [17] STAR Collab., L. Adamczyk *et al.*, Phys. Rev. **D86** (2012) 032006.
- [18] J. C. Collins and D. E. Soper, Nucl. Phys. **B194** (1982) 445.
- [19] A. Bacchetta, F. Conti and M. Radici, Phys. Rev **D78** (2008) 074010.

- [20] M. Burkhardt, *Nuovo Cimento* **35C N2** (2012) 261.
- [21] M. Göckeler *et al.*, *Phys. Rev. Lett.* **98** (2007) 222001.
- [22] A. Bacchetta, M. Diehl, K. Goeke, A. Metz, P. Mulders and M. Schlegel, *JHEP* **0702** (2007) 093.
- [23] HERMES Collab., A. Airapetian *et al.*, *Phys. Lett.* **693** (2010) 11.
- [24] COMPASS Collab., M.G. Alekseev *et al.*, *Phys. Lett.* **B692** (2010) 240.
- [25] COMPASS Collab., F. Bradamante, *Nuovo Cimento* **35C N2** (2012) 107.
- [26] COMPASS Collab., M.G. Alekseev *et al.*, *Phys. Lett.* **B673** (2009) 127.
- [27] JLAB HallA Collab., X. Qian *et al.*, *Phys. Rev. Lett.* **107** (2011) 072003.
- [28] BELLE Collab., R. Seidl *et al.*, *Phys. Rev.* **D78** (2008) 032011.
- [29] BABAR Collab., I. Garzia, *Nuovo Cimento* **35C N2** (2012) 79.
- [30] M. Anselmino *et al.*, *Phys. Rev.* **D75** (2007) 054032; *Nucl. Phys.* **B191** (2009) 98.
- [31] HERMES Collab., A. Airapetian *et al.*, *JHEP* **0806** (2008) 017.
- [32] COMPASS Collab., C. Adolf *et al.*, *Phys. Lett.* **B713** (2012) 10.
- [33] BELLE Collab., A. Vossen *et al.*, *Phys. Rev. Lett.* **107** (2011) 072004.
- [34] M. Radici, *Nuovo Cimento* **35C N2** (2012) 69.
- [35] A. Vossen, *Nuovo Cimento* **35C N2** (2012) 59.
- [36] HERMES Collab., A. Airapetian *et al.*, *Phys. Rev. Lett.* **103** (2009) 152002.
- [37] M. Anselmino, M. Boglione and S. Mellis, [arxiv:1204.1239 \[hep-ph\]](#)
- [38] M. Anselmino *et al.*, *Phys. Rev.* **D79** (2009) 054010.
- [39] A. Bacchetta and M. Radici, *Phys. Rev. Lett.* **107** (2011) 212001.
- [40] HERMES Collab., M. Contalbrigo, *AIP Conf. Proc.* **1388** (2011) 471.
- [41] COMPASS Collab., G. Sbrizzai, *Nuovo Cimento* **35C N2** (2012) 129.
- [42] COMPASS Collab., B. Parsamyan, *J. Phys. Conf. Ser.* **295** (2011) 012046.
- [43] HERMES Collab., L. L. Pappalardo, *AIP Conf. Proc.* **1441** (2012) 229.
- [44] JLAB HallA Collab., J. Huang *et al.*, *Phys. Rev. Lett.* **108** (2012) 052001.